J. Biochem. 2021;0(0):1–15 doi:10.1093/jb/mvab016

JB THE JOURNAL OF BIOCHEMISTRY

Inhibition of flippase-like activity by tubulin regulates phosphatidylserine exposure in erythrocytes from hypertensive and diabetic patients

Received September 28, 2020; accepted February 9, 2021; published online February 12, 2021

Tamara Muhlberger[1,*,†], Melisa Micaela Balach[1,2,†], Carlos Gastón Bisig[3], Verónica Silvina Santander[1,2], Noelia Edith Monesterolo[1,2], Cesar Horacio Casale[1,2] and Alexis Nazareno Campetelli[1,2,+]

[1]Departamento de Biología Molecular, Facultad de Ciencias Exactas, Físico-Químicas y Naturales, Universidad Nacional de Río Cuarto, Ruta Nacional 36, km 601, Río Cuarto, 5800 Córdoba, Argentina; [2]INBIAS CONICET-UNRC. Instituto de Biotecnología Ambiental y Salud. Campus UNRC, Río Cuarto, Córdoba, Argentina; and [3]Centro de Investigaciones en Química Biológica de Córdoba (CIQUIBIC), UNC-CONICET, Departamento de Química Biológica, Facultad de Ciencias Químicas, Universidad Nacional de Córdoba, Ciudad Universitaria, 5000 Córdoba, Argentina

*Present address: UNITEFA–CONICET, Departamento de Farmacia, Facultad de Ciencias Químicas. Universidad Nacional de Córdoba, Ciudad Universitaria, 5000 Córdoba, Argentina
†These authors made equal contributions to this study.ORCID ID: 0000-0003-2552-8103
+Alexis N. Campetelli, Departamento de Biología Molecular, Facultad de Ciencias Exactas, Físico-Químicas y Naturales, Universidad Nacional de Río Cuarto, Ruta Nacional 36, km 601, Río Cuarto, 5800 Córdoba, Argentina. Tel.: +54-358-4676422, Fax: +54-358-4676232, email: acampetelli@exa.unrc.edu.ar

Plasma membrane tubulin is an endogenous regulator of P-ATPases and the unusual accumulation of tubulin in the erythrocyte membrane results in a partial inhibition of some their activities, causing hemorheological disorders like reduced cell deformability and osmotic resistance. These disorders are of particular interest in hypertension and diabetes, where the abnormal increase in membrane tubulin may be related to the disease development. Phosphatidylserine (PS) is more exposed on the membrane of diabetic erythrocytes than in healthy cells. In most cells, PS is transported from the exoplasmic to the cytoplasmic leaflet of the membrane by lipid flippases. Here, we report that PS is more exposed in erythrocytes from both hypertensive and diabetic patients than in healthy erythrocytes, which could be attributed to the inhibition of flippase activity by tubulin. This is supported by: (i) the translocation rate of a fluorescent PS analog in hypertensive and diabetic erythrocytes was slower than in healthy cells, (ii) the pharmacological variation of membrane tubulin in erythrocytes and K562 cells was linked to changes in PS translocation and (iii) the P-ATPase-dependent PS translocation in inside-out vesicles (IOVs) from human erythrocytes was inhibited by tubulin. These results suggest that tubulin regulates flippase activity and hence, the membrane phospholipid asymmetry.

Graphical Abstract

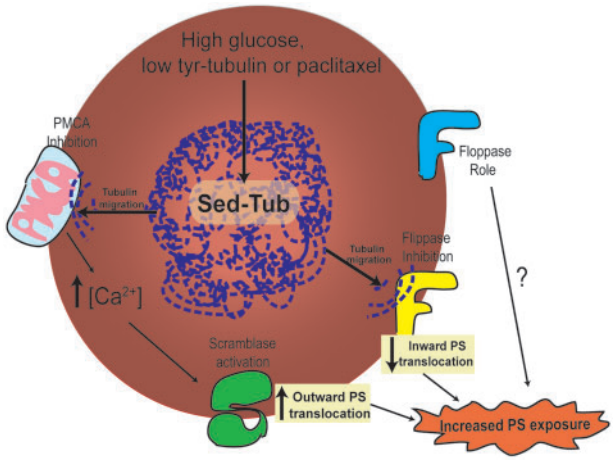

Keywords: diabetes; erythrocytes; hypertension; phosphatidylserine; tubulin.

Abbreviations: AChE, acetylcholinesterase; ANOVA, analysis of variance; EDTA, ethylenediaminetetraacetic acid; FBS, foetal bovine serum; IOV, inside-out vesicle; NBD-PS, 1-palmitoyl-2-{6-[(7-nitro-2-1,3-benzoxadiazol-4-yl)amino]hexanoyl}-*sn*-glycero-3-phosphoserine; PBS, phosphate buffer saline; PBS-G, phosphate-buffered saline with glucose; PE, phycoerythrin; PKC, protein kinase C; PMCA, plasma membrane calcium ATPase; PS, phosphatidylserine; SD, standard deviation; SDS–PAGE, sodium dodecyl sulphate–polyacrylamide gel electrophoresis.

In previous research, we described how P-ATPases are inhibited when they become associated with tubulin, the microtubule protein. This conserved mechanism (*1*–*4*) is of remarkable importance in erythrocytes from subjects with some pathologies which feature increased membrane tubulin, such as diabetes and hypertension (*1*, *5*–*7*).

In a retrospective cohort study conducted to estimate the incidence rates of new-onset hypertension

in adult cancer patients, Fraeman *et al*. observed that approximately one-third of adult cancer patients developed recent-onset hypertension a few weeks after starting chemotherapy, without a prior history of it (*8*). Tumour type was a major factor in the incidence of different grades of hypertension, subjects with gastric and ovarian cancer, which are conventionally treated with Paclitaxel, experienced the highest incidence of severe hypertension (*9*). We have previously shown that the administration of Paclitaxel in Wistar rats resulted in arterial hypertension. This drug promotes the migration of tubulin from a sedimentable fraction to the plasma membrane of erythrocytes, which in turn inhibits Na^+-K^+, and Ca^{2+}-ATPase activity and thus leads to poor cell deformability and reduced osmotic resistance, among other effects (*1*, *5*, *6*, *10*, *11*). The impairment in deformability, in particular, creates a vicious rheological cycle: the abnormal erythrocyte passage in the microvasculature causes mechanical damage to the stagnant erythrocyte membrane, insufficient oxygen delivery and tissue hypoxia. The result is further vasoconstriction and blood pressure elevation (*12*). Another contributing factor to the development of hypertension might be that Paclitaxel impairs endothelium-dependent vasorelaxation (*13*).

Patients treated with Paclitaxel, moreover, showed a high prevalence of deep vein thrombosis and pulmonary embolism (*9*). Kim *et al*. found that Paclitaxel intravenous administration significantly promoted venous thrombosis *in vivo* (*14*). The effect of Paclitaxel on thrombosis, however, is not well understood. These authors also showed that Paclitaxel could induce phosphatidylserine (PS) exposure *ex vivo* in erythrocytes and partially attributed it to a PKCζ-mediated scramblase activation, but the rest of the puzzle is yet to be completed (*14*). This paper looked into the putative inhibitory effect of tubulin on the P4-ATPase family of aminophospholipid translocases and thus into its involvement in PS exposure, since this family has some functional and structural homology with type II and III P-ATPase members. We found that erythrocytes from diabetic and hypertensive subjects, where plasma membrane tubulin is increased (*1*, *6*, *10*), have more exposed PS than healthy erythrocytes as a result of a delayed inward PS translocation rate. Furthermore, we observed that the incorporation of the added PS analog, NBD-PS (1-palmitoyl-2-{6-[(7-nitro-2-1,3-benzoxadiazol-4-yl)amino]hexanoyl}-*sn*-glycero-3-phosphoserine (NBD-PS) by cells can be pharmacologically modulated by Paclitaxel and Nocodazole. Finally, *in vitro* assays of flippase activity showed that tubulin inhibits the flipping of NBD-PS in IOVs from human erythrocytes.

Materials and Methods

Materials

Chemicals, antibodies and culture media were from Sigma-Aldrich (St. Louis, MO, USA) unless otherwise stated. IR Dye 800CW goat anti-mouse IgG was from Li-Cor Biosciences (Lincoln, NE, USA). PS fluorescent analog NDB-PS was from Avanti Polar Lipids. Foetal bovine serum (FBS) was from Internegocios (Buenos Aires, Argentina). FluorSave was from Calbiochem (Billerica, MA, USA).

Human subjects and erythrocyte preparation

Male and female patients (aged between 25 and 60) were recruited as blood donors at the Regional Hospital in Río Cuarto, Córdoba, Argentina. Patient selection and blood extraction were performed in compliance with relevant laws and institutional guidelines, using an informed consent protocol approved by the Committee on Research Ethics (CoEdi) of the National University of Río Cuarto, consistent with the standards in the Declaration of Helsinki.

Fresh blood samples were collected in Vacutainer tubes (Becton–Dickinson; Plymouth, UK), with ethylenediaminetetraacetic acid (EDTA; 1 mg/ml) as anticoagulant (*15*). Erythrocytes were obtained by conventional centrifugal separation and used immediately. Fasting glucose level was analysed in the samples through the glucose oxidase method after a 14-h fast and considering the haemoglobin A1C level, which reflects glycosylation of the haemoglobin molecule. Haemoglobin A1C had been measured during the preceding 8–12 weeks to assess overall metabolic control. Diabetic patients were selected on the basis of specific criteria, including blood glucose concentration >150 mg/dl and haemoglobin A1C (HbA1C) higher than 7%. On the other hand, a personal history of consistent blood pressure equal to or higher than 160/110 mmHg was taken into account for selecting hypertensive subjects. Subjects characteristics are summarized in Table I. Individuals with both, diabetes and hypertension were discarded.

Animals

Wistar rats used in this study were bred at our university bioterium and maintained in an air-conditioned room (21 ± 1°C) with controlled lighting (12h/12h light/dark cycle). They were anesthetized by inhalation with isoflurane and euthanized by decapitation. Pelleted food and tap water were available *ad libitum*. All the animals were carefully monitored and kept in accordance with the recommendations by the local Research Ethics Committee (CoEDi).

Cell culture

HEK293T cells were cultured in Dulbecco's Modified Eagle's - Medium (DMEM) supplemented with 10% (v/v) FBS, 10 units ml^{-1}

Table I. Patients conditions and characteristics

	Control		Diabetic		Hypertensive	
	M	F	M	F	M	F
No of patients	6	9	8	8	8	8
Age (years)	42 ± 13	42 ± 14	44 ± 12	48 ± 12	47 ± 7	58 ± 7
RBC count (× 10^6/μl)	5.1 ± 0.5	4.5 ± 0.3	5.1 ± 0.7	4.8 ± 0.4	5 ± 0.5	4.6 ± 0.3
HGT (g/cL)	15.3 ± 1	13.3 ± 0.9	15 ± 2.3	13.4 ± 0.8	15.6 ± 0.7	13.5 ± 1.1
HTC (%)	45.4 ± 3.2	40.3 ± 3.7	45.3 ± 7.1	41.2 ± 3.4	45.6 ± 2.9	40.5 ± 4
Weight (kg)	72.8 ± 10	62 ± 5.2	80.5 ± 10.6	68.2 ± 5.5	83 ± 13	67 ± 6.7
SBP (mmHg)	125 ± 11	128 ± 13	122 ± 15	132 ± 10	161 ± 18*	157 ± 16*
DBP (mmHg)	85 ± 9	88 ± 6	90 ± 7	87 ± 8	103 ± 8*	101 ± 12*
Fasting plasma glucose (mg/dl)	80 ± 5	78 ± 8	163 ± 12*	165 ± 14*	83 ± 6	86 ± 7

*$P < 0.05$ versus control.

penicillin and 100 $\mu g ml^{-1}$ streptomycin. All of them were maintained at 37°C in a humidified 5% CO_2 atmosphere.

K562 cells were cultured in Roswell Park Memorial Institute - Medium (RPMI) supplemented with 10% (v/v) FBS, 10 units ml^{-1} penicillin and 100 $\mu g ml^{-1}$ streptomycin. All of them were maintained at 37°C in a humidified 5% CO_2 atmosphere.

IOVs from human erythrocytes

The protocol first described by Steck *et al.* was performed in its entirety at 4°C to obtain the vesicles (*16*). Specifically, human erythrocytes were lysed in 40 vol of 5P8 buffer (5 mM NaH_2PO_4, pH 8) and the resulting ghosts were washed three times with the same buffer. Vesicularization was started by suspension of the ghost fraction in 0.5P8 buffer (0.5 mM NaH_2PO_4, pH 8) for 15 h. Resealed vesicles were collected by centrifugation at 28,000 × g for 20 min, resuspended in 1 ml 0.5P8 buffer, vortexed thoroughly and finally passed through a 27-gauge needle to complete vesicularization. The vesicle mixture was loaded on a Dextran 87 barrier (lower phase, δ: 1.09, upper phase, δ: 1.03) and centrifuged in a SW41 rotor at 200,000 × g for 2 h. IOVs were rescued from the interphase, while inside-in and unsealed vesicles remained in the pellet. Finally, the IOV fraction was washed by dilution to 40 ml in 0.5P8 buffer and centrifuged at 28,000 × g for 30 min.

Sidedness assay

The IOVs were assessed considering the inaccessibility of markers found on the exterior of the intact erythrocyte [*i.e.* acetylcholinesterase (AChE)]. Surfactants were used to disrupt the permeability barrier and expose the latent marker. AchE activity was assayed following the method described by Ellman *et al.* (*17*). Briefly, 15 µl IOVs (2-10 µg of protein) were preincubated in cuvettes with an equal volume of 5P8 or Triton X-100. The reaction mixture (0.4 mM acetylthiocholine, 0.33 mM 5,5 dithiobis-2-nitrobenzoic acid and 100 mM sodium phosphate, pH 7.5) was added to make 0.5 ml, and the reaction was followed spectrophotometrically at 412 nm at room temperature. Activity in the presence of Triton X-100 indicated total AchE activity, while activity in the absence of Triton X-100 indicated the percentage of inside-in vesicles and permeable membranes.

In vitro *NBD-PS translocation assay*

About 60 µg IOVs (per reaction tube) were loaded with 3 µM NBD-PS by incubation for 5 min in ice-cold water. Then, the IOV-NBD-PS mixture was centrifuged at 22,000 × g for 15 min at 4°C to remove unloaded NBD-PS. The pellets (loaded IOVs) were resuspended in 0.5P8 buffer (120 µl final volume). For o-Vanadate inhibition experiments, 1 mM o-Vanadate was added 15 min before the start of the reaction. For tubulin inhibition experiments, tubulin in Mes-EGTA-Magnesium Buffer (MEM buffer) (100 mM Mes, pH 6.7, containing 0.1 mM Ethylene glycol tetraacetic acid (EGTA) and 1 mM $MgCl_2$, which gives mostly nonpolymerized tubulin) was added 15 min before the reaction started to obtain the following increasing tubulin concentrations: 0, 75, 150, 350, 500 and 700 µg/ml. The reaction was started by transferring reaction samples from 4°C to a 30°C water bath, with the addition of 10 mM ATP and 10 mM $MgCl_2$. At the indicated times, 20 µl of the reaction mixture were taken, added with 15 µl 3% Bovine serum albumin (BSA) (fatty acid free grade) and incubated at 4°C for 5 min. Then, 350 µl 0.5P8 buffer were added and the samples were centrifuged at 22,000 × g. The supernatants were carefully removed and added with 800 µl 0.5P8 supplemented with 0.1% Triton X-100 to dissolve any NBD-PS aggregation. NBD fluorescence, which was determined in a Fluoromax-3 spectrofluorimeter (Horiba Instruments Inc.) using λ_{ex}: 467 nm and λ_{em}: 534 nm, was proportional to the NBD-PS on the extra vesicle side.

Tubulin preparations

Rat brain tubulin preparations were isolated as previously described (*18*). Briefly, brains from 30- to 60-day-old male Wistar rats were homogenized at 4°C in 1 volume MEM buffer containing 1 mM $MgCl_2$. The homogenate was centrifuged at 100,000 × g for 45 min, and the pellet was discarded. Tubulin was purified over two cycles of assembly/disassembly, followed by phosphocellulose chromatography.

Sodium dodecyl sulphate–polyacrylamide gel electrophoresis (SDS–PAGE) and immunoblotting

Proteins were separated by SDS–PAGE on 12% polyacrylamide slab gel with the Laemmli method (*19*), and the gel was transferred to a nitrocellulose sheet. Blots were reacted with mAb DM1A (anti α-tubulin, dilution 1:1,000) and 5F10 [anti-pam-plasma membrane calcium ATPase (PMCA), dilution 1:1,000]. The sheet was reacted with the corresponding peroxidase-conjugated anti-IgG antibody and stained by the 4-chloro-1-naphthol method or the ECL system. Band intensities were quantified using FIJI-ImageJ® (National Institutes of Health, MD, USA).

Protein determination

Protein concentration was determined by the Bradford method (*20*).

In cells NBD-PS translocation assay

Flippase activity was assayed by flow cytometry: 1 µl of 1 mg/ml NBD-PS was added to 1 ml suspension of washed erythrocytes (5% hematocrit) or 5×10^5 cells of the K562 cell line in phosphate-buffered saline with glucose (PBS-G), and incubated for 5 min at 10°C. Cells were then centrifuged to discard unadsorbed NBD-PS and resuspended in 500 µl PBS-G. Immediately after transferring the reaction tubes to a 37°C water bath [for K562 cells the water bath was programed at 18°C to minimize endocytic incorporation of the fluorescent phospholipids (*21*)] (time 0), and after 20 min of incubation (time 20), aliquots (1×10^5 cells) were either washed with 900 µl of PBS-G or PBS-G supplemented with 1% BSA (fatty acid free grade) to remove NBD-PS remaining in the outer leaflet. Finally, the cells were resuspended in 500 µl of PBS-G. NBD-PS derived fluorescence was immediately measured by flow cytometry, and the percentage of NBD-PS in the extracellular leaflet was calculated as the fluorescence difference between PBS-G washed cells (100% NBD-PS fluorescence) and PBS-G plus 1% BSA washed cells (% of internalized NBD-PS). For each assay, 30,000 events were counted.

PS exposure

Cells were washed three times with ice-cold HPS (145 mM NaCl, 7.5 mM KCl, 10 mM glucose and 10 mM Hepes, pH 7.4) supplemented with 2 mM $CaCl_2$ by centrifugation (20 s, 12,000 × g). Approximately 1×10^6 cells were incubated with 1 µl Annexin-V-PE (BD Biosciences®) in 100 µl Annexin binding buffer containing 145 mM NaCl, 2.5 mM $CaCl_2$,10 mM HEPES, pH 7.4, for 15 min at room temperature in the dark. After incubation, each sample was added with 400 µl binding buffer and the samples were kept in ice for further analysis by cell cytometry using a Guava EasyCyte (EMB, Millipore) flow cytometer. Annexin-V binding was measured with an excitation wavelength of 488 nm and an emission wavelength in the yellow spectrum. A marker (M1) was placed to set an arbitrary threshold between Annexin-V binding cells and unlabelled cells. A dot plot of forward scatter versus side scatter was set at linear scale for both parameters. At least three different blood samples were used for each experiment and 30,000 events counted for each sample.

IOV-tubulin coprecipitation

IOVs (60 µg) were incubated with different concentrations of tubulin in 600 µl 0.5P8 buffer for 1 h at 37°C. Then, the suspension was centrifuged at 20,000 × g for 30 min and the pellet was washed with 0.5P8 buffer. The pellets were resuspended in Laemmli sample buffer (*19*) and tubulin content was determined by western blot using DM1A antibody.

Immunofluorescence

HEK293T cells were transiently double-transfected by the polyethylenimine method with plasmids p-hATP11C/pCAG-HAC (containing the HA-tagged ATP11C gene) and p-hCDC0-pcDNA3-HFN (containing the FLAG-tagged CDC50A gene), kindly provided by Professor Hye-Won Shin from Kyoto University. Transfected cells were grown on coverslips. The coverslips were incubated with Alexa FluorTM 594 wheat agglutinin for 10 min at room temperature. Cells were then fixed with 4% P/V paraformaldehyde and 3% P/V sucrose for 15 min at 37°C, and permeabilized with 0.1% V/V Triton X-100 in PBS for 10 min at room temperature. Then, the cells were washed three times for 5 min with PBS and incubated with a blocking solution containing 3% P/V BSA in PBS for 1 h at

37°C. Next, they were incubated overnight at 4°C with the monoclonal primary antibodies anti-DM1A and anti-HA, in a 1:1,000 dilution in PBS with 1% BSA. After a 3× PBS wash, the cells were incubated for 1 h at room temperature with the secondary antibodies Alexa Fluor® 488 and Alexa Fluor®633 in 1:1,000 dilutions in PBS with 1% P/V BSA. Finally, the samples were washed with PBS three times for 5 min and all the preparations were mounted using the FluorSave mounting medium. Images were collected using an Olympus FV1200 spectral confocal microscope (Olympus Latin America, Miami, FL, USA) equipped with an argon/helium/neon laser at the corresponding wavelength on the software (Olympus FV Viewer) provided by the manufacturer, and processed on the FIJI-ImageJ® program (Wayne Rasband; NIH, USA) using the colocalization threshold plug-in to calculate Pearson's coefficients.

Plasma membrane preparation

Erythrocytes isolated from 2 ml human blood were resuspended in 3 ml lysis buffer [7.5 mM sodium phosphate, pH 7.5, containing 1 mM EDTA and 20 mg/ml phenylmethylsulfonyl fluoride (PMSF)] and incubated for 15 min. The lysate was centrifuged at 20,000 × g for 20 min. The pellet was washed three times with 6 ml lysis buffer without PMSF, resuspended in 3 ml lysis buffer and stored at −20°C until use.

K562 cells cultured in T25 flasks (~1×10^6 cells) were harvested and washed three times with PBS. The harvested cells were resuspended in 1 ml ice-cold distilled water (supplemented with 5 mg/ml PMSF), and stirred for 30 min in ice. The suspension was homogenized in a glass Dounce homogenizer and centrifuged at 3,000 × g for 1 min. The supernatant was centrifuged at 48,000 × g for 25 min and washed with PBS buffer. The pellet was resuspended in 0.1 ml PBS buffer and used immediately.

Statistical analysis

All the images, including western blots, are representative of at least three independent experiments. Flow cytometric assays were performed in triplicate, and each experiment was repeated several times. The data are presented as the mean ± standard deviation (SD) of at least three independent experiments. Analysis of variance (ANOVA) with Fisher post hoc test and Student's *t*-test were used. Differences were considered statistically significant when $P < 0.05$.

Results

Increased PS exposure in erythrocytes from hypertensive and diabetic subjects

Previously, we showed that membrane tubulin is higher in erythrocytes from hypertensive (H) and diabetic (D) subjects than in healthy controls (C), as a result of tubulin translocation from a sedimentable fraction located in the cytoplasm. Membrane tubulin inhibits NKA and PMCA and thus causes changes in some rheological properties, such as decreased cell deformability and reduced osmotic resistance (*1*, *5*, *6*, *11*). Since flippases also belong to the P-ATPase superfamily, we proposed that tubulin might also inhibit this enzyme. Flippase inhibition would in turn result in PS accumulation on the extracellular side of the membrane. To verify this, the amount of endogenous PS exposed on the erythrocyte membrane was quantified using the Annexin-V-PE method and cell cytometry in healthy, diabetic and hypertensive subjects. When we analysed Annexin-V positive cells, the PS exposure was found to be 29.1% and 31.6% higher in erythrocytes from hypertensive and diabetic subjects, respectively, than in healthy ones (fluorescence mean values for erythrocytes labelled with Annexin-V-PE) (Fig. 1a, bars). This difference did not originate from erythrocytes auto fluorescence since erythrocytes from several patients did not show any statistically relevant difference (not shown) and furthermore, it has been described that auto fluorescence in erythrocytes from diabetic mouse is even lower than in healthy controls (*22*). The apparent mismatch between the histogram plot (Fig. 1a, up) and the bar graph (Fig. 1a, bottom) comes from an increased number of highly Annexin-V positive cells (PS++) in hypertensive patients (11.5% versus 4.93% in diabetic and 1.5% in control subjects, Fig. 1b). PS asymmetry, therefore, was effectively altered in these erythrocytes featuring increased plasma membrane tubulin (Fig. 1c).

In order to understand the origin of the PS accumulation in these cells, we then determined the translocation rate of the PS fluorescent analog NBD-PS. The 'out to in' PS translocation is an enzymatic process that is carried out by flippases and follows a Michaelian kinetics. The NBD-PS translocation is lineal for around 25 min and translocates around 72% of the added NBD-PS after 1 h (Fig. 1d). To assay the NBD-PS translocation rate, erythrocytes from normal, diabetic and hypertensive subjects were loaded with NBD-PS and then incubated for 20 min at 37°C with NBD-PS. The NBD-PS remaining on the outer leaflet was extracted with 1% BSA at time 0 and after 20 min at 37°C (a period of time that guarantees initial velocity conditions), in such a way that the remaining cell-associated fluorescence (quantified by flow cytometry) represented PS that had been flipped into the inner leaflet. Figure 1e shows the fluorescence percentage in the extracellular leaflet after 20 min. As expected, erythrocytes from both hypertensives and diabetic subjects had a substantially higher percentage of NBD-PS on the extracellular side of the membrane (15% and 18%, respectively), which suggests inhibited PS translocation to the intracellular side. This means that tubulin could perturb flippase activity *in vivo*, since increased plasma membrane tubulin was related to lower flippase activity.

Regulation of PS flipping in erythrocytes and K562 erythroid cell line by plasma membrane tubulin

The amount of free tubulin, microtubules or tubulin associated with the plasma membrane in a cell can be pharmacologically regulated. In earlier , we found that some drugs that affect microtubules are also able to modify the levels of membrane tubulin. Nocodazole, for instance, removes tubulin from the membrane, while Paclitaxel induces its association (*10*, *11*). To ascertain whether endogenous tubulin inhibits flippase activity *in vivo*, erythrocytes were incubated for 45 min with these two drugs, as well as with o-Vanadate (a potent P-ATPase inhibitor) and a combination of both Paclitaxel and o-Vanadate, and then loaded with NBD-PS. We then quantified the NBD-PS fluorescence percentage in the extracellular leaflet. After 20 min, >40% of the NBD-PS was flipped in control cells and only 18% in o-Vanadate-treated cells, which highlights the importance of P-ATPase flipping activity when it comes to uptaking exposed PS (Fig. 2a).

When membrane-associated tubulin was higher, *i.e.* in Paclitaxel-treated cells (Fig. 2b, upper panel), 20%

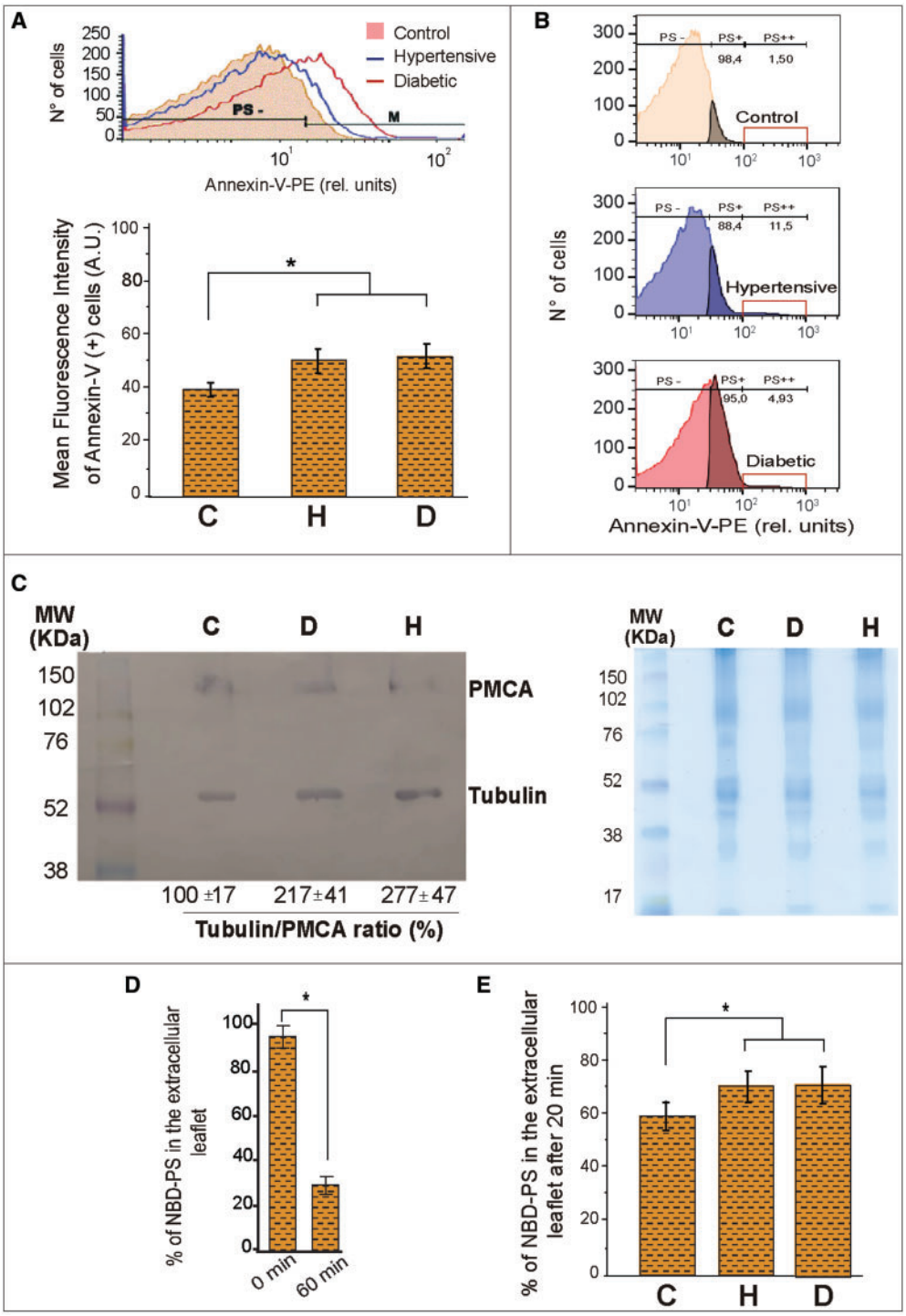

Fig. 1. PS exposure in erythrocytes from healthy, diabetic and hypertensive subjects. (**a**) Endogenous PS exposure was quantified in erythrocytes from healthy [control (C)], diabetic (D) and hypertensive (H) subjects by flow cytometry analysis using Annexin-V-PE and counting 30,000 events in each experiment. The mean fluorescence intensity of the Annexin-V positive cells population is observed (bottom). An original histogram representative of several experiments of the erythrocytes marked with Annexin-V-PE is shown in the upper panel. (**b**) Annexin-V positive cells were sub classified in PS+ (overlapping) and PS++ (red box) (the latter having a fluorescence of one logarithm greater than PS+). The percentage of cells that were in each group was determined. Original histograms representative of several experiments (*n*: 3 for each kind of patient) are shown. (**c**) Upper panel: Plasma membrane fractions were obtained from 2 ml human blood as described in Materials and Methods section. An aliquot of each fraction was processed for immunoblot analysis with antibodies against α-tubulin and PMCA (as an internal control). The result from a typical experiment is shown. Tubulin bands were quantified using ImageJ and the Tubulin/PMCA ratio is indicated. Bottom panel: a representative SDS gel stained with Coomassie Brilliant Blue is shown to confirm that the same amount of proteins was loaded in each line. (**d**) Erythrocytes from healthy (control) subjects were added with 3 μM NBD-PS and incubated in ice-cold water for 5 min. After incubation, remaining NBD-PS was removed by centrifugation at 1,000 × g. Finally, the cells were transferred to a water bath at 37°C, and at times 0 and 60 min the exposed NBD-PS was back extracted and the translocated NBD-PS was quantified by flow cytometry (30,000 cells of each blood sample were analysed). (**e**) Erythrocytes from healthy (control), diabetic and hypertensive subjects were treated as in d but the NBD-PS translocation was determined at time 0 and 20 min. Values are the mean ± SD from three independent experiments. (*) reflects statistically significant differences (ANOVA with Fisher test, $P < 0.05$, Freedom degree = 2 and $F > 8$).

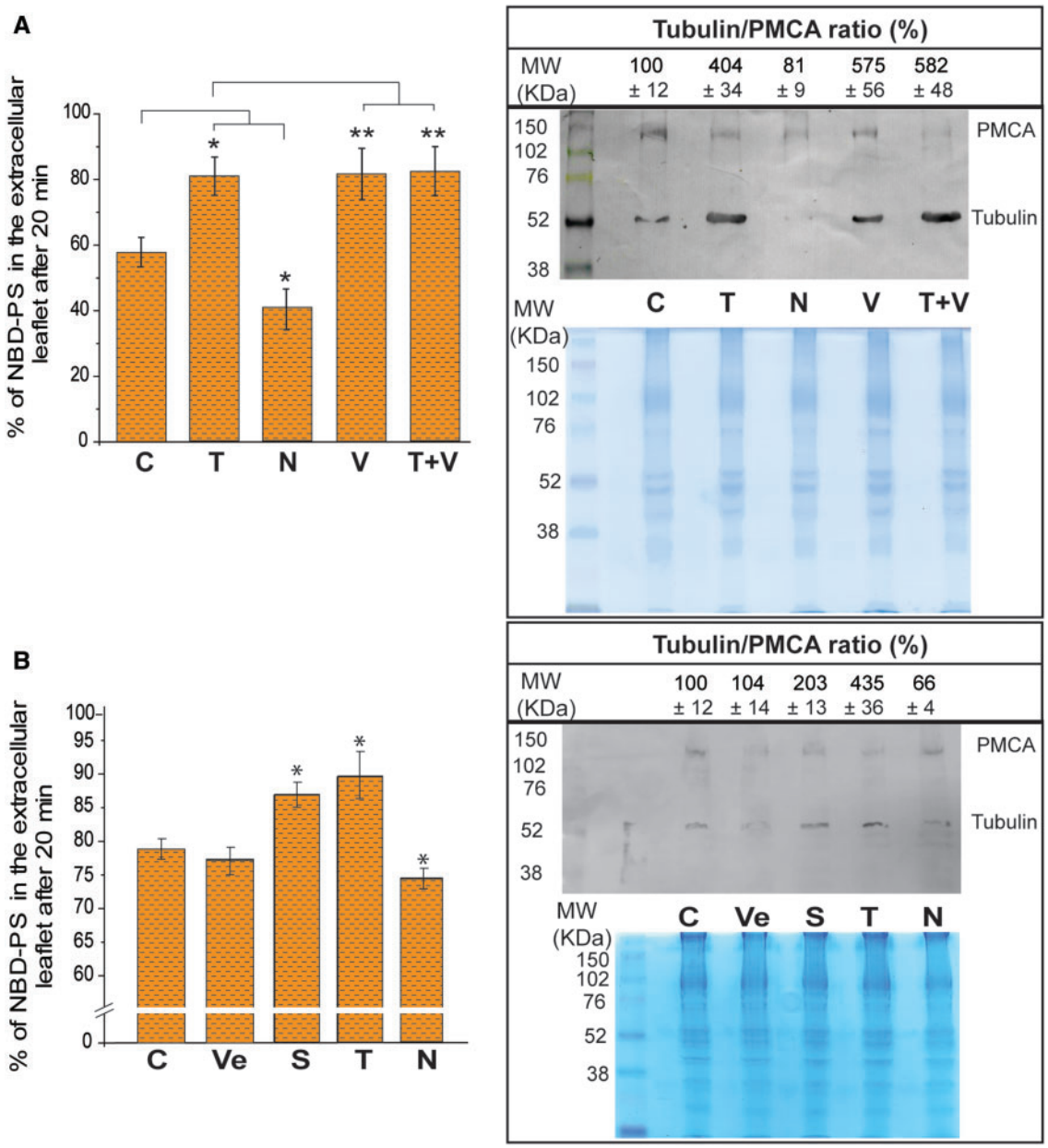

Fig. 2. Modulation of NBD-PS translocation by membrane tubulin *in vivo*. (**a**) (Left) Erythrocytes from healthy subjects [control (C)] were incubated with 7 μM Paclitaxel (T), 50 μM Nocodazole (N), 200 μM o-Vanadate (V) and Paclitaxel + o-Vanadate (T + V). (**b**) (Left) K562 cells [control (C)] were incubated with ethanol [control vehicle (Ve)], Hank's solution (S), 7 μM Paclitaxel (T) and 50 μM Nocodazole (N) for 30 min at 37°C. After treatments, cells were incubated with NBD-PS. For times 0 and 20 min, the exposed NBD-PS was back extracted and quantified by flow cytometry as was described in Materials and Methods section. The values are the mean ± SD from three independent experiments. (*) reflects statistically significant differences (versus C) and (**) reflects nonstatistically significant differences (versus T). ANOVA with Fisher test, $P < 0.05$, Freedom degree = 3 and $F > 7$. (a and b, right panels) Plasma membrane fractions were obtained from human erythrocytes (a) and K562 cells (b) as described in Materials and Methods section. An aliquot of each fraction was processed for SDS–PAGE to confirm equal amount of proteins in each gel line (bottom) and subjected to immunoblot analysis with antibodies against α-tubulin and PMCA (as an internal control) (up). The result from a typical experiment is shown. Tubulin and PMCA bands were quantified using ImageJ and the Tubulin/PMCA ratio is indicated (*2*).

of the fluorescent analog was flipped (Fig. 2a), indicating a reduction in flippase activity. By contrast, Nocodazole-treated cells featuring reduced membrane tubulin had a higher NBD-PS translocation percentage than the control (58%), which indicates flippase activation. The treatment with both Paclitaxel and o-Vanadate at the same time served to rule out a possible activation of floppases by tubulin in cells treated only with Paclitaxel, since the combination of both drugs did not increase the exposed NBD-PS in comparison with o-Vanadate on its own. All these results suggest the presence of a flippase activity regulated by tubulin that contributes to the asymmetrical distribution of PS in the membrane of human erythrocytes.

Flippase activity was also assayed in the lineage related K562 cell line, since there is a marked difference in cytoskeleton composition between

erythrocytes and nucleated mammalian cells. Similar results were obtained, with Paclitaxel-treated cells flipping only 12% of the probe, half of what control cells did (Fig. 2c). A similar behaviour was observed in starved cells (treated with Hank's solution), for which we found increased tubulin in the plasma membrane (unpublished results) (Fig. 2d). However, flippase inhibition under this condition could be mostly attributed to ATP depletion. Conversely, Nocodazole treatment resulted in a mild increase in flipped NBD-PS. As expected, plasma membrane tubulin content was modulated by Nocodazole and Paclitaxel in these cells, too (Fig. 2d, upper panel).

In general, effects of Nocodazole and Paclitaxel observed in K562 cells were similar to those observed in erythrocytes, although less pronounced. This could be due to several factors. For instance, the dynamism of microtubules (which are absent in erythrocytes) could be disturbed in the K562 cells and thus affect lipid flippase activity, as was previously described for another enzyme (*7*). Moreover, endocytosis has been found to uptake flippase ATP11C and the drugs used could be altering this process (*23*).

Still, since the possibility of a direct effect of the drugs on flipping activity needed to be excluded, we looked into the localization of tubulin and ATP11C on the plasma membrane. HEK293T cells were transiently transfected with a combination of HA-tagged ATP11C and an N-terminally FLAG-tagged CDC50A construct, which is a chaperone involved in the proper localization of ATP11C at the plasma membrane (plasmids p-hATP11C/pCAG-HAC and p-hCDC0-pcDNA3-HFN, respectively). The cualitative confocal microscopy images (Fig. 3a) were quantitatively analysed with the Colocalization Threshold plug-in (FIJI) to calculate the Pearson correlation coefficients between tubulin (green) and ATPC11 (red) signals. This quantitative measure estimates the degree of overlap between fluorescence signals obtained in two channels (*24*). Higher Pearson values represent a higher degree of colocalization of two signals, ranging from 1 (maximal colocalization) to −1 (no colocalization) (*25*). Figure 3b displays Pearson's coefficient for untreated cells (control), cells treated with Paclitaxel or Nocodazole, and for cells starved in Hank's solution. In control cells, values for Pearson's coefficient were disperse (wide box) since there is a heterogeneous population of cells with different amount of tubulin in the plasma membrane. In cells treated with Paclitaxel, Pearson's coefficient had a media of 0.45 which indicate a higher colocalization between both proteins. Since the amount of ATP11C in the membrane was not altered under this condition (Fig. 3c), the result confirmed that tubulin in these cells was induced to associate to the membrane, and therefore that membrane tubulin (and not an alteration in microtubule dynamism) was responsible for the behaviour of flippase activity in K562 cells. Conversely, Pearson's coefficient in Nocodazol-treated cells was 0.21 (with a compact box) indicating that less tubulin was associated with the plasma membrane (see *Merge* and *Merge MP* in Fig. 3a and compare Paclitaxel versus Nocodazole treatment), and

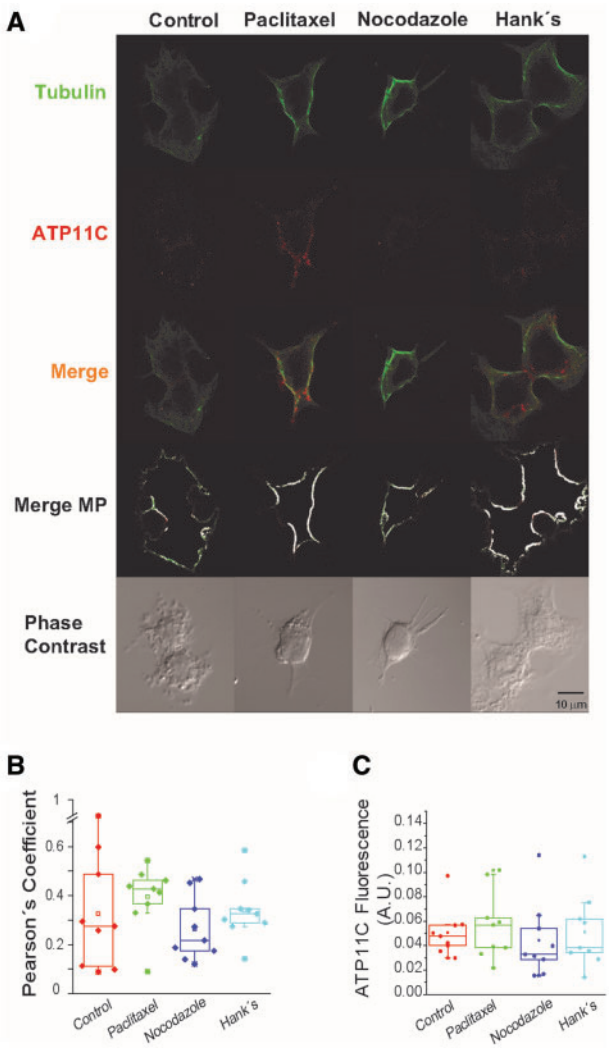

Fig. 3. Tubulin and ATP11C colocalizates in the plasma membrane of HEK293T cells. (**a**) A cualitative colocalization analysis was performed in HEK293T cells treated for 1 h with Paclitaxel (10 μM), Nocodazole (50 μM) and Hank's solution. Cells were fixed and immunostained with Alexa-488 (ATP11C-HA and Alexa-633 (DM1A, α-Tubulin). Merge MP displays the colocalization of both proteins in a mask that only included the plasma membrane. (**b**) Box plot of the Pearson's correlation coefficients that were calculated using the FIJI software from *z*-stacks of four images each and *n*: 10. Statistical properties of data shown in box plot are as follows: mean (Open Square), box (25/75% quantile), asterisks (1/99% quantile) and whiskers (maximum and minimum). (**c**) The amount of ATP11C was quantified in the plasma membrane of HEK293T cells by confocal microscopy using FIJI, *n*: 9 for each condition and same statistical properties as in b.

supporting the results observed in Fig. 2b. In Hank's treated cells, it is observed an intermediate behaviour between Paclitaxel- and Nocodazole-treated cells, which correlate with the blot observed in Fig. 2b, suggesting that the poor flippase activity can be explained in part by an increase of membrane tubulin (not as high as in Paclitaxel-treated cells), an also by limited ATP availability.

Figure 3c shows that content of ATP11C was not changed under any tested condition, which rules out the involvement of membrane endocytosis. Taken together, these results suggest that membrane tubulin

regulates flippase activity *in vivo* not only in erythrocytes but also in other cells; however, it is premature to assign a direct inhibitory effect of tubulin on flippases since PMCA is also inhibited by tubulin, and an intracellular Ca^{2+} increase may occur, positioning Ca^{2+} as the real inhibitor (discussed below).

Inhibition of P-ATPase-dependent PS translocation by tubulin in inside-out erythrocyte vesicles

Results showed before reveals a correlation between membrane tubulin content and PS flipping and a colocalization between the P-ATPase ATP11C and tubulin when the last is translocated to the membrane. Moreover, as was mentioned above, tubulin modulates the activity of certain P-ATPases in several cells and tissues (*2*, *4*, *18*), as well as in human and rat erythrocytes (*10*, *11*). We therefore proposed that tubulin might also affect the activity of ATP11C, a major flippase described for human erythrocytes (*26*). To confirm this, we assessed flippase activity *in vitro* and evaluated the effect of tubulin.

Phospholipid asymmetry in the plasma membrane is maintained and regulated mainly by ATP-driven flippases and floppases (*27*, *28*). While flippases specifically transport PS and PE from the extracellular leaflet of the membrane to the cytoplasmic side, floppases transport phospholipids and other compounds in the opposite direction, from the cytoplasmic leaflet to the extracellular side, with less specificity (Fig. 4a). Flippase activity has been previously assayed *in vitro* through either BSA (fatty acid free) back extraction or the dithionite assay method, in proteoliposomes (*29*, *30*), isolated organelles (*31*) and intact cells (*32*, *33*). To assay flippase activity *in vitro* in the proper lipidic enzyme environment, we considered inverting the orientation of the erythrocyte plasma membrane. The sealed, IOVs of erythrocytes, which result from erythrocyte lysis and a subsequent recircularization step performed at low ionic strength and slightly alkaline pH, were a good fit for this purpose: they expose the ATP-active cytosolic side and thus phospholipid exchange in and out of them is inverted (Fig. 4b). This makes it possible to overcome the limited access to ATP and guarantees a proper orientation of enzymes in the membrane, the accessibility of substrates and effectors and a conserved phospholipidic environment that avoids reconstitution artefacts (*34*).

Upon addition of the fluorescent PS analog NBD-PS to an IOV suspension in ice, most of the probe was incorporated into the exposed cytosolic leaflet (the extravesicular side) of the bilayer and pelleted with the membranes when centrifuged at high speed. However, if the membranes with intercalated NBD-PS were incubated with BSA before centrifugation, nearly 100% of the probe was back extracted and remained in the supernatant (Fig. 4c). This means that the probe was accessible to BSA and must have resided on the extra vesicular side. Incubation of the labelled membranes at 37°C allowed for a slow passive redistribution of the probe from the extra to the intravesicular leaflet over time (measured in hours, Fig. 4c).

IOVs were prepared from blood samples taken from healthy donors, following the protocol described by Steck (*16*). The population of vesicles generated through this procedure is mostly made up of inside-out forms, but a small percentage of inside-in and unsealed vesicles remain as contaminants. Unsealed vesicles can negatively impact the flippase assay, since BSA is then able to access both sides of the membrane and accuracy is reduced. The percentage of IOVs in our preparation was determined by measuring AChE activity (a sidedness marker assay), as described by Ellman *et al.* (*17*). Typically, 85–95% IOVs were obtained (Fig. 4d), a percentage that should not affect accuracy. On the other hand, IOVs are very unstable structures that can be disrupted by temperature, ionic strength, pH variations or other physical issues. To check how stable their structure was when NBD-PS or tubulin was added, AChE activity was assessed. As can be observed in Fig. 4e and f, the addition of the probe or different concentrations of tubulin did not affect vesicle stability.

Flippase activity was assessed next. Different amounts of IOVs were incubated with an excess of NBD-PS and the amount of NBD-PS remaining in the cytosolic leaflet (the extravesicular side) was quantified by spectrofluorometry using the BSA back-extraction method (*35*). In the absence of ATP, the probe was not translocated to the intravesicular side for times as long as 60 min, even at the highest IOV concentrations (Fig. 5a). Instead, the presence of ATP brought about a decrease in NBD-PS on the extravesicular side, and as expected, this change was dependent on IOV content. Under our experimental conditions, the maximum percentage of translocated NBD-PS did not exceed 20% (Fig. 5b), and translocation was linear for up to 30 min for an IOV content of between 40 and 60 μg of proteins. With a higher content, linearity was lost. These results show that under our experimental conditions, NBD-PS translocation was an enzymatic process that remained linear for 30 min, when both ATP and IOVs (40–60 μg of proteins) were included. The decrease in NBD-PS on the extravesicular side can be attributed to a higher rate of PS transport to the intravesicular leaflet mediated by floppases, and to a slower rate of flippases in the opposite direction. As both enzymes translocate phospholipids in reverse directions (Fig. 4a and b), flippase inhibition means the action of floppases is not counterbalanced and there are higher rates of PS transport into the vesicle.

This was further confirmed when the IOVs were incubated with o-Vanadate, which is known to strongly inhibit P-type ATPases (*36*). In effect, incubation with 1 mM of the drug was associated with a marked decrease in NBD-PS on the extravesicular side (Fig. 6a). The linearity observed in the absence of o-Vanadate was missing, and the translocation of 20% of the probe into the membrane was achieved in 15 min, half the time registered without the drug.

Finally, we analysed the effect of increasing concentrations of purified tubulin on ATP-dependent NBD-PS translocation in IOVs. In the absence of tubulin, 91% of the probe was detected on the extravesicular side after 15 min of reaction. The addition of exogenous tubulin, on the other hand, decreased NBD-PS

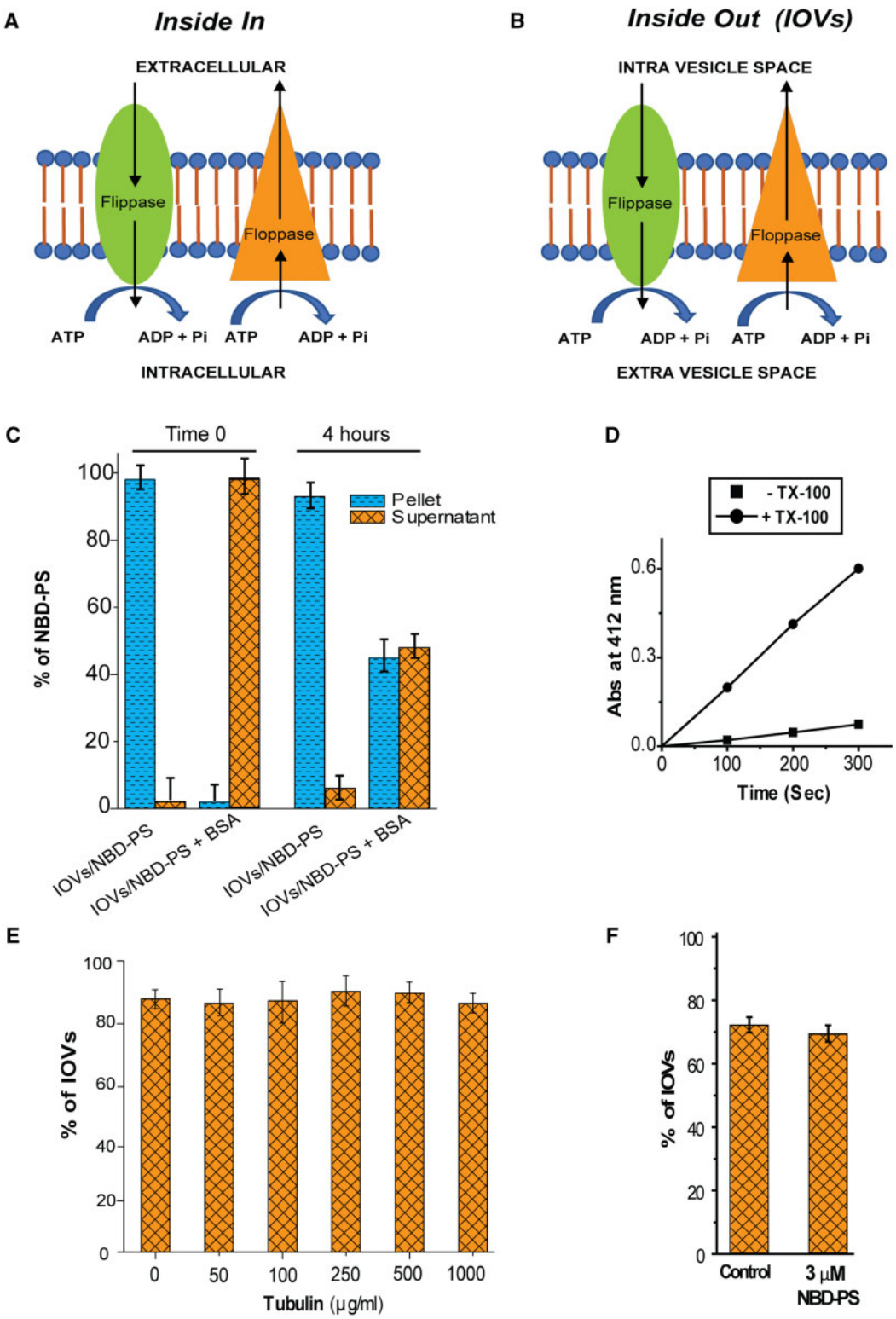

Fig. 4. Cells versus IOVs enzyme orientation and time-dependent NBD-PS distribution. (**a**) The diagram depicts the localization of flippases and floppases in the plasma membrane of a cell (inside-in). In both enzymes, the ATP-active sites are intracellular and flippases translocate PL from the exoplasmic to the cytoplasmic side of the membrane, while floppases work in the reverse direction. (**b**) In IOVs, the ATP-active sites for both enzymes become exposed, but the translocation direction remains unaltered. Cytosolic components are now exposed. (**c**) To evaluate the time-dependent NBD-PS distribution in IOVs, IOVs from human erythrocytes were loaded with 3 µM NBD-PS, and incubated at 37°C at the times indicated. NBD-PS was back extracted (+BSA) or not (−BSA) as described in Materials and Methods section, and NBD-PS fluorescence was determined in the pellet and supernatant fraction. (**d**) Determination of IOV percentage obtained from human erythrocytes. AChE activity was determined as explained in Materials and Methods section, in the presence (total activity) and absence (inside-in activity) of Triton X-100. The difference between the total activity and the inside-in activity corresponds to the IOV percentage. (**e**) Effect of Tubulin on IOV stability. 30 µg IOVs (total proteins) were preincubated for 30 min at 37°C with increasing amounts of purified rat brain tubulin. An aliquot was then used to measure AChE activity as described in Materials and Methods section. (**f**) Effect of NBD-PS on IOV stability. Approximately 60 μg vesicles were incubated for 1 h at 37°C with 3 µM NBD-PS. AChE activity was determined in the vesicles and IOV percentage was calculated.

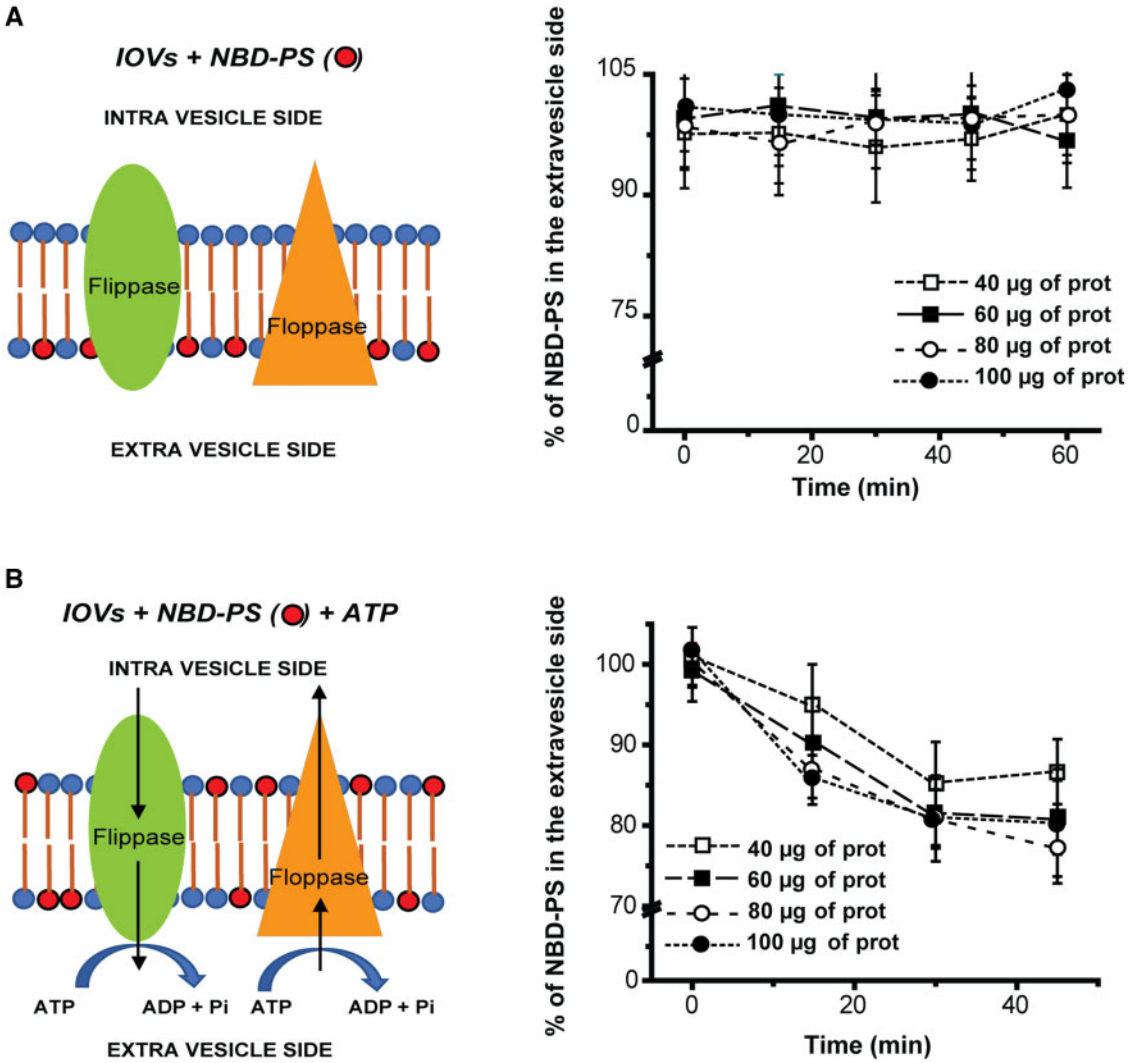

Fig. 5. Determination of flippase activity *in vitro*. (**a**) IOV suspensions (40, 60, 80, 100 µg of total proteins) were supplemented with 3 µM NBD-PS. The probe was intercalated on the extravesicular side of the membrane and remained there for >60 min. No probe translocation was observed at increased IOV concentrations (right panel). (**b**) IOVs (40, 60, 80, 100 µg of total proteins) supplemented with 3 µM NBD-PS were incubated in the presence of 10 mM ATP. The NBD-PS percentage on the extra vesicle side was determined spectrofluorometrically as described in Materials and Methods section. Values are the mean ± SD from three independent experiments, including several biological replicates (different IOV preparations) and three technical replicates.

translocation from the intravesicular side to the extravesicular side, in a concentration-dependent manner (Fig. 6b). The maximum inhibition was observed with 350 µg/ml tubulin, since additional tubulin did not seem to produce any supplemental inhibition. While the concentration of tubulin necessary to completely inhibit the flippase *in vitro* seems unattainable under cellular conditions, the fact that under certain conditions tubulin accumulates in the plasma membrane, the place where flippases reside, results in the concentration of tubulin a significant number of times, explaining the effect observed *in vitro*. It is unclear how the *in vitro* inhibition of flippases by tubulin occurs, but there is a direct correlation between the inhibition and the amount of exogenous tubulin associated to the plasma membrane (Fig. 6c). This experiment also ruled out that the flippase inhibition observed in *in vivo* experiments can be attributed to a Ca^{2+} increase mediated by PMCA inhibition, since Ca^{2+} ions were absents in these experiments. Interestingly, full flippase inhibition was reached with 350 µg/ml of tubulin, a concentration close to that at which the binding between IOVs and tubulin reached saturation. At higher tubulin concentrations, some tubulin polymerization may occur and give rise to sedimentable microtubules. However, we could not sediment tubulin by centrifugation (20,000 × g) in control experiments in the absence of IOVs (data not shown). Moreover, we were also able to rule out a direct effect of microtubule-affecting drugs on flippase activity, since ATP-dependent NBD-PS translocation in the vesicles was not affected in the presence of Paclitaxel and Nocodazole (Fig. 6d).

Although the precise mechanism through which tubulin inhibits flippases *in vitro* is unclear, the degree of inhibition and the amount of exogenous membrane associated tubulin are certainly correlated (Fig. 6c). This strongly suggests that tubulin is able to inhibit

P-ATPase flipping activity in the erythrocyte plasma membrane, and that it may therefore be considered a new regulator of phospholipid symmetry.

Discussion

In certain pathologies, like arterial hypertension and diabetes, there is an increased level of membrane tubulin in erythrocytes. Erythrocytes from diabetic patients are also believed to have more exposed PS than normal ones, and this has been linked to increased erythrocyte adhesion to the endothelium, and subsequent microvasculature occlusion (*37*). Our results not only confirmed this but also indicated a similar behaviour in erythrocytes from hypertensive subjects (Fig. 1a). Furthermore, we found that the rate of PS translocation in both diabetic and hypertensive erythrocytes was reduced (Fig. 1e), which means there is a correlation between increased PS exposure and membrane tubulin in these two cases. A putative inhibitory effect of tubulin on lipid flipping was evaluated *in vivo* through experiments where membrane tubulin content was pharmacologically altered. The two drugs chosen were Nocodazole, a well-known antineoplastic agent that interferes with microtubule polymerization, and Paclitaxel, a microtubule-stabilizing drug. Both are commonly used to either deplete or intensify the microtubular network, respectively. In previous research, we showed that Nocodazole removes tubulin from the membrane while Paclitaxel does the exact opposite, inducing its association (*10*). As can be seen in Fig. 2, the new *in vivo* assays showed that tubulin indeed modulated the translocation of the fluorescent PS analog, NBD-PS, from the extracellular to the intracellular leaflet. In comparison with the control, PS was translocated faster in Nocodazole-treated cells and significantly more slowly in Paclitaxel-treated cells. In other words, a high PS exposure seems to be a consequence of high membrane tubulin and not an independent event, similar to what was observed with other tubulin-regulated P-ATPases (*2*, *4*, *18*). Since it is flippase that translocate PS from the external to the cytosolic surface of the cell, tubulin might then be inhibiting flippase activity.

The results of the assays with o-Vanadate, a known potent P-ATPase inhibitor, pointed in the same direction: flippase activity inhibition in this case was very similar to that observed under Paclitaxel treatment. The possibility that this could be attributed to floppase activation by tubulin was ruled out, since coincubation with Paclitaxel plus o-Vanadate did not increase PS exposure (Fig 2). Kim *et al*. attributed the increase in PS exposure they observed in Paclitaxel-treated erythrocytes to an increase in PKCζ-mediated scramblase activity and in intracellular Ca^{2+} (*14*). However, our experiments in erythrocyte IOVs demonstrated that Ca^{2+} is dispensable, since it only took the presence of tubulin for PS translocation to be reduced (Fig. 6). Furthermore, the Paclitaxel concentration chosen by Kim *et al*., which was five times greater than the one used in our experiments and in cancer therapies (*38–40*), can cause other effects such as echinosytosis and even eryptosis, which may result in anaemia (*41*). Curiously, none of these studies was careful to observe the influence of tubulin in erythrocytes. PKCζ-mediated scramblase activity, besides, could only be partially inhibited by PKCζ inhibitors, so other pathways must be involved in Paclitaxel-induced PS exposure (*14*).

On the other hand, sickle-shaped erythrocytes incubated with the PKCζ activator PMA (Phorbol Myristate Acetate) showed a twofold increase in scramblase activity with respect to normal erythrocytes incubated with the same drug, but PS exposure was almost four times greater in the normal erythrocytes (*42*). This demonstrates that PS exposure does not depend mainly on scramblase activity. Not surprisingly, PMA, much like Paclitaxel, also induces tubulin polymerization (*43*), which supports our hypothesis that membrane-associated tubulin inhibits flippase activity.

A similar behaviour was observed for tubulin in the erythroid cell line K562. Paclitaxel and Nocodazole treatment, as well as starvation, also made it possible to regulate the amount of membrane-bound tubulin in these cells (Figs 2b and 3a and b). A directly proportional correlation was found here between the amount of tubulin in the plasma membrane and PS exposure: the higher the content of membrane-associated tubulin, the greater the PS exposure and vice versa. These results reveal that PS flipping is modulated by tubulin *in vivo*, and that tubulin needs to be associated with the plasma membrane to fulfil its inhibitory function. A clean *in vitro* experiment confirmed this inhibitory effect. Flippase activity was assayed using erythrocyte IOVs, NBD-PS as a substrate, and ATP as the energy supply. The addition of purified tubulin to the reaction mixture inhibited the flipping activity, since NBD-PS translocation from the extra to the intravesicular side significantly decreased with the addition of tubulin to the reaction mixture, which means that tubulin was acting as a flippase inhibitor.

Since PS exposure on the cell surface fulfils a critical role in events like apoptosis, sperm capacitation, platelet activation and others, when unregulated it may result in early apoptosis or spontaneous platelet activation and must therefore be precisely controlled. One of the most common side effects found in cancer patients treated with Paclitaxel is anaemia (*44*, *45*). In these patients, this blood disorder was associated with an increase of intracellular Ca^{2+} and a parallel activation of sphingomyelinase with the subsequent formation of ceramide. Together, Ca^{2+} and ceramide induce scramblase activation and lead to PS exposure. The erythrocytes affected by the process are finally cleared from the circulating blood (*41*). However, as mentioned before, Paclitaxel-induced PS exposure in erythrocytes cannot be explained only by scramblase activation (*46–48*).

Other vascular malignancies have been related to Paclitaxel administration, including stroke, deep vein thrombosis and pulmonary embolia. Thrombus formation is a complex event where PS exposure both in platelets and erythrocytes plays a central role. Exacerbated exposure could facilitate undesirable

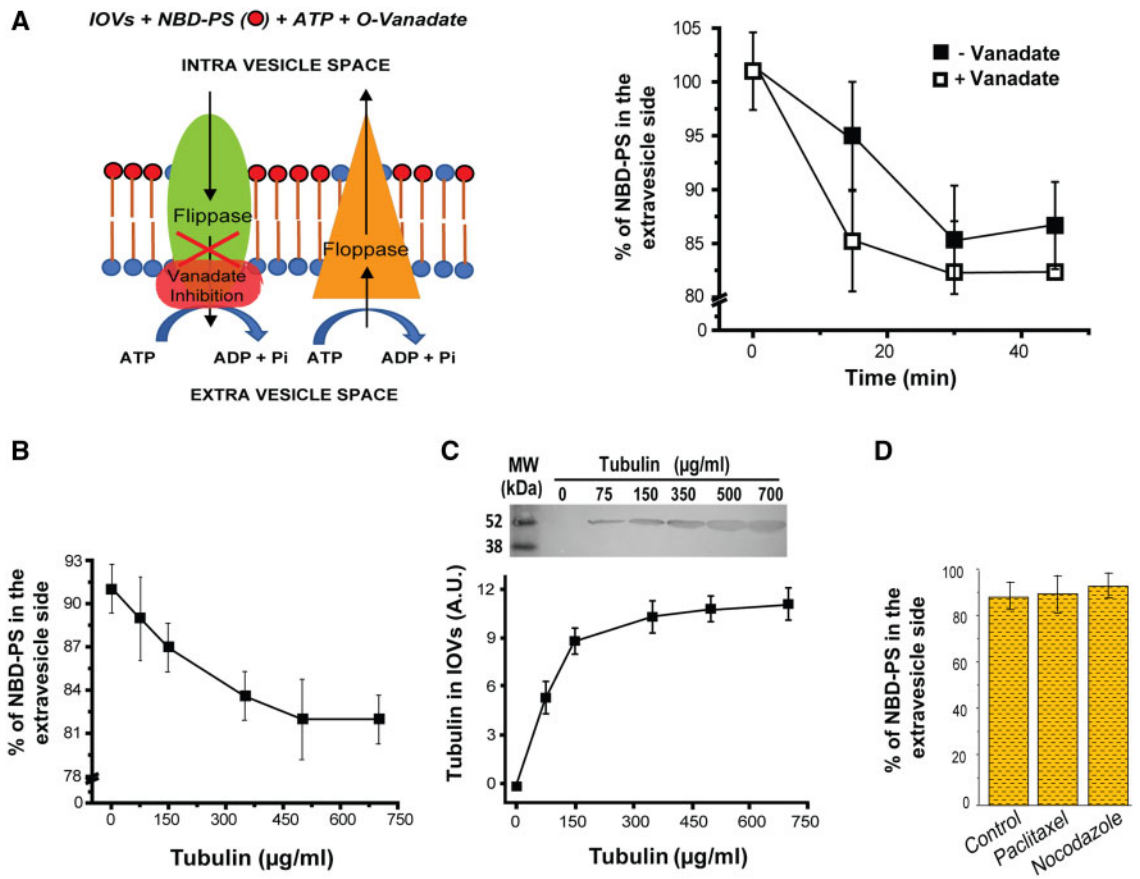

Fig. 6. Tubulin inhibits a flippase-like activity in erythrocyte IOVs. (**a**) Left panel: the diagram depicts the assay system. Right panel: 40 µg IOVs (330 µg ml of total proteins) were loaded with 3 µM NBD-PS and pre incubated with (□) or without (■) 1 mM o-Vanadate for 15 min at 4°C. Finally, 10 mM ATP was added and the mixture was transferred to a water bath at 30°C and the NBD-PS percentage on the extra vesicle side was recorded across time as described in Materials and Methods section. (**b**) About 40 µg IOVs (330 µg ml of total proteins) were loaded with 3 µM NBD-PS and pre incubated for 20 min at 30°C with increasing amounts of purified rat brain tubulin. Finally, 10 mM ATP was added and the NBD-PS percentage remaining on the extra vesicle side after 15 min of reaction at 30°C was determined. (**c**) 60 µg IOVs (total proteins) were pre incubated for 30 min at 37°C with increasing amounts of purified rat brain tubulin. The suspension was centrifuged at 20,000 × g for 20 min at 4°C and the pellets were resolved by SDS–PAGE. Tubulin was detected using specific DM1A antibody. Bands corresponding to tubulin were quantified using ImageJ software. (**d**) IOVs (60 µg total proteins) supplemented with 3 µM NBD-PS were incubated with Paclitaxel (10 μM) and Nocodazole (50 μM) and added with 10 mM ATP. The mixture was then transferred to a water bath at 30°C and after 20 min, the NBD-PS percentage on the extra vesicle side was determined. For a, b and d, the NBD-PS percentage on the extra vesicle side was determined spectrofluorometrically as described in Materials and Methods section and the values are the mean ± SD from three independent experiments, including several biological replicates (different IOVs preparations) and three technical replicates. The blot in c is a representative sample of three independent experiments.

thrombi formation, thus increasing the risk of vascular occlusion which becomes relevant in the COVID-19 pandemic, where coagulopathies like hypercoagulability are the hallmark of severe outcomes (*49*) and where hypertension and diabetes are the most usual associated comorbidities (*50*). Healthy individuals may also be affected: 0.5% of their erythrocytes expose PS (a number equivalent to 20% of platelets), and since erythrocytes participate in the formation of venous thrombi, it would only take a small 0.5% increase to raise their risks of developing clots.

Our study describes an alternative mechanism behind PS exposure in Paclitaxel-treated cells: tubulin associates with the plasma membrane thanks to the action of the drug, inhibits the activity of lipid flippases which should carry PS into the cell, and thus induces PS exposure on the outer surface. In the membrane, tubulin also inhibits PMCA (*4*) and therefore increases intracellular Ca^{2+} levels [as observed by Lang *et al.* (*41*)]. As a result of this increase, flippases are also inhibited (*51*), and at a much higher Ca^{2+} concentration scramblases are activated (*52*) (Fig. 7). The mild PS exposure observed in diabetic and hypertensive erythrocytes may be due to tubulin-mediated flippase inhibition, while scramblase activation may be driving the rampant PS exposure occurring during platelet activation or apoptosis, where high intracellular Ca^{2+} is pivotal. Clearly, PS exposure can be triggered by more than one pathway, in a hierarchical fashion.

The fact that tubulin induces flippase inhibition should not be taken in account only in cancer patients being treated with Paclitaxel. There are two other groups of risk, diabetics and hypertensive patients. In these patients, tubulin is subject to membrane migration, either due to high glucose in the first case (*7*, *53*) or the lack of tubulin tyrosination in the second case (*5*, *10*) (Fig. 7). These pathologies, then, might also

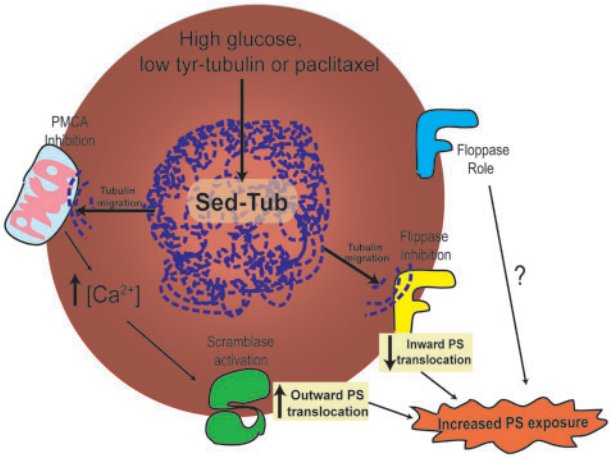

Fig. 7. Model of PS exposure regulation by tubulin in erythrocytes. Migration of tubulin to the plasma membrane in erythrocytes, either in pathological situations as diabetes or arterial hypertension or by paclitaxel treatment results in flippase and PMCA (among other P-ATPases) inhibition. There is a direct mild PS exposure due to flippases inhibition that can be transformed in an enhanced PS exposure when the $[Ca^{2+}]_i$ threshold for scramblase activation is overpassed as a result of PMCA inhibition. The role of lipid floppases in this proposed mechanism is uncertain.

feature flippase inhibition and the alteration of other P-ATPase activities, which might impair hemorheological properties like cell deformability and osmotic resistance and thus impact normal blood flow. The involvement of erythrocytes tubulin should be considered when attempting to elucidate the underlying factors that contribute to diabetes-associated anaemia and the occurrence of a hypercoagulable state in hypertension, two complications that have long been imperfectly understood.

Conclusion

Our finding that tubulin associated to the plasma membrane inhibits PS flipping and thus contributes to its exposure on the cell surface introduces a novel flippase regulation mechanism that has significant implications in pathologies like hypertension and diabetes. Further analyses will be necessary to understand exactly how tubulin is able to participate in the generation or maintenance of plasma membrane phospholipid asymmetry, as well as its role in processes that involve breaking PS asymmetry, such as eryptosis, clot formation and others.

Acknowledgements

We would like to thank Pr Hye-Won Shin from Kyoto University for sharing ATP11C and CDC50 plasmids, and Florencia Sgarlatta for editing the language of the manuscript and Pamela Gaich from Regional Hospital in Río Cuarto for blood sample supplying.

Funding

The study was supported by grants from Agencia Nacional de Promoción Científica y Tecnológica de la Secretaría de Ciencia y Tecnología del Ministerio de Cultura y Educación as part of the Programa de Modernización Tecnológica (PICT 00-00000-0826/12 (Dr Casale), 2205/15 (Dr Campetelli)), Consejo Nacional de Investigaciones Científicas y Técnicas (CONICET) (Dr Casale), Secretaría de Ciencia y Técnica de la Universidad Nacional de Río Cuarto (Dr Casale) and Ministerio de Industria, Comercio, Minería y Desarrollo Científico Tecnológico de la Provincia de Córdoba (Dr Campetelli).

Conflict of Interest

None declared.

References

1. Amaiden, M.R., Monesterolo, N.E., Santander, V.S., Campetelli, A.N., Arce, C.A., Pie, J., Hope, S.I., Vatta, M.S., and Casale, C.H. (2012) Involvement of membrane tubulin in erythrocyte deformability and blood pressure. *J. Hypertens.* **30**, 1414–1422
2. Campetelli, A.N., Previtali, G., Arce, C.A., Barra, H.S., and Casale, C.H. (2005) Activation of the plasma membrane H-ATPase of *Saccharomyces cerevisiae* by glucose is mediated by dissociation of the H(+)-ATPase-acetylated tubulin complex. *FEBS J.* **272**, 5742–5752
3. Casale, C.H., Previtali, G., and Barra, H.S. (2003) Involvement of acetylated tubulin in the regulation of Na+,K+-ATPase activity in cultured astrocytes. *FEBS Lett.* **534**, 115–118
4. Monesterolo, N.E., Santander, V.S., Campetelli, A.N., Arce, C.A., Barra, H.S., and Casale, C.H. (2008) Activation of PMCA by calmodulin or ethanol in plasma membrane vesicles from rat brain involves dissociation of the acetylated tubulin/PMCA complex. *FEBS J.* **275**, 3567–3579
5. Amaiden, M.R., Santander, V.S., Monesterolo, N.E., Nigra, A.D., Rivelli, J.F., Campetelli, A.N., Pie, J., and Casale, C.H. (2015) Effects of detyrosinated tubulin on Na+,K+-ATPase activity and erythrocyte function in hypertensive subjects. *FEBS Lett.* **589**, 364–373
6. Nigra, A.D., Monesterolo, N.E., Rivelli, J.F., Amaiden, M.R., Campetelli, A.N., Casale, C.H., and Santander, V.S. (2016) Alterations of hemorheological parameters and tubulin content in erythrocytes from diabetic subjects. *Int. J. Biochem. Cell Biol.* **74**, 109–120
7. Rivelli, J.F., Amaiden, M.R., Monesterolo, N.E., Previtali, G., Santander, V.S., Fernandez, A., Arce, C.A., and Casale, C.H. (2012) High glucose levels induce inhibition of Na,K-ATPase via stimulation of aldose reductase, formation of microtubules and formation of an acetylated tubulin/Na,K-ATPase complex. *Int. J. Biochem. Cell Biol.* **44**, 1203–1213
8. Fraeman, K.H., Nordstrom, B.L., Luo, W., Landis, S.H., and Shantakumar, S. (2013) Incidence of new-onset hypertension in cancer patients: a retrospective cohort study. *Int. J. Hypertens.* **2013**, 1–10
9. Herrmann, J. (2020) Vascular toxic effects of cancer therapies. *Nat. Rev. Cardiol.* **17**, 503–522
10. Amaiden, M.R., Santander, V.S., Monesterolo, N.E., Campetelli, A.N., Rivelli, J.F., Previtali, G., Arce, C.A., and Casale, C.H. (2011) Tubulin pools in human erythrocytes: altered distribution in hypertensive patients affects Na+, K+-ATPase activity. *Cell. Mol. Life Sci.* **68**, 1755–1768
11. Monesterolo, N.E., Nigra, A.D., Campetelli, A.N., Santander, V.S., Rivelli, J.F., Arce, C.A., and Casale, C.H. (2015) PMCA activity and membrane tubulin affect deformability of erythrocytes from normal and

hypertensive human subjects. *Biochim. Biophys. Acta* **1848**, 2813–2820
12. Kaczmarska, M., Fornal, M., Messerli, F.H., Korecki, J., Grodzicki, T., and Burda, K. (2013) Erythrocyte membrane properties in patients with essential hypertension. *Cell Biochem. Biophys.* **67**, 1089–1102
13. Vassilakopoulou, M., Mountzios, G., Papamechael, C., Protogerou, A.D., Aznaouridis, K., Katsichti, P., Venetsanou, K., Dimopoulos, M.A., Ikonomidis, I., and Papadimitriou, C.A. (2010) Paclitaxel chemotherapy and vascular toxicity as assessed by flow-mediated and nitrate-mediated vasodilatation. *Vascul. Pharmacol.* **53**, 115–121
14. Kim, K., Chang, Y.K., Bian, Y., Bae, O.N., Lim, K.M., and Chung, J.H. (2018) Pro-Coagulant and Pro-Thrombotic Effects of Paclitaxel Mediated by Red Blood Cells. *Thromb. Haemost.* **118**, 1765–1775
15. Nguyen, D.B., Wagner-Britz, L., Maia, S., Steffen, P., Wagner, C., Kaestner, L., and Bernhardt, I. (2011) Regulation of phosphatidylserine exposure in red blood cells. *Cell Physiol. Biochem.* **28**, 847–856
16. Steck, T.L. and Kant, J.A. (1974) Preparation of impermeable ghosts and inside-out vesicles from human erythrocyte membranes. *Methods Enzymol.* **31**, 172–180
17. Ellman, G.L., Courtney, K.D., Andres, V. Jr., and Feather-Stone, R.M. (1961) A new and rapid colorimetric determination of acetylcholinesterase activity. *Biochem. Pharmacol.* **7**, 88–95
18. Casale, C.H., Alonso, A.D., and Barra, H.S. (2001) Brain plasma membrane Na+,K+-ATPase is inhibited by acetylated tubulin. *Mol. Cell. Biochem.* **216**, 85–92
19. Laemmli, U.K. (1970) Cleavage of structural proteins during the assembly of the head of bacteriophage T4. *Nature* **227**, 680–685
20. Bradford, M.M. (1976) A rapid and sensitive method for the quantitation of microgram quantities of protein utilizing the principle of protein-dye binding. *Anal. Biochem.* **72**, 248–254
21. Suzuki, J., Umeda, M., Sims, P.J., and Nagata, S. (2010) Calcium-dependent phospholipid scrambling by TMEM16F. *Nature* **468**, 834–838
22. Fauaz, G., Miranda, A.R., Gomes, C.Z., Courrol, L.C., Silva, F.R., Rocha, F.G., Schor, N., and Bellini, M.H. (2010) Erythrocyte protoporphyrin fluorescence as a potential marker of diabetes. *Appl. Spectrosc.* **64**, 391–395
23. Takatsu, H., Takayama, M., Naito, T., Takada, N., Tsumagari, K., Ishihama, Y., Nakayama, K., and Shin, H.W. (2017) Phospholipid flippase ATP11C is endocytosed and downregulated following Ca(2+)-mediated protein kinase C activation. *Nat. Commun.* **8**, 1423
24. Zinchuk, V., Zinchuk, O., and Okada, T. (2007) Quantitative colocalization analysis of multicolor confocal immunofluorescence microscopy images: pushing pixels to explore biological phenomena. *Acta Histochem. Cytochem.* **40**, 101–111
25. Zinchuk, V., Wu, Y., and Grossenbacher-Zinchuk, O. (2013) Bridging the gap between qualitative and quantitative colocalization results in fluorescence microscopy studies. *Sci. Rep.* **3**, 1365
26. Arashiki, N., Takakuwa, Y., Mohandas, N., Hale, J., Yoshida, K., Ogura, H., Utsugisawa, T., Ohga, S., Miyano, S., Ogawa, S., Kojima, S., and Kanno, H. (2016) ATP11C is a major flippase in human erythrocytes and its defect causes congenital hemolytic anemia. *Haematologica* **101**, 559–565
27. Andersen, J.P., Vestergaard, A.L., Mikkelsen, S.A., Mogensen, L.S., Chalat, M., and Molday, R.S. (2016) P4-ATPases as phospholipid flippases-structure, function, and enigmas. *Front. Physiol.* **7**, 275
28. Bevers, E.M. and Williamson, P.L. (2016) Getting to the outer leaflet: physiology of phosphatidylserine exposure at the plasma membrane. *Physiol. Rev.* **96**, 605–645
29. Malvezzi, M., Chalat, M., Janjusevic, R., Picollo, A., Terashima, H., Menon, A.K., and Accardi, A. (2013) Ca2+-dependent phospholipid scrambling by a reconstituted TMEM16 ion channel. *Nat. Commun.* **4**, 2367
30. Vehring, S., Pakkiri, L., Schröer, A., Alder-Baerens, N., Herrmann, A., Menon, A.K., and Pomorski, T. (2007) Flip-flop of fluorescently labeled phospholipids in proteoliposomes reconstituted with *Saccharomyces cerevisiae* microsomal proteins. *Eukaryot. Cell* **6**, 1625–1634
31. Natarajan, P. and Graham, T.R. (2006) Measuring translocation of fluorescent lipid derivatives across yeast Golgi membranes. *Methods* **39**, 163–168
32. Pomorski, T., Muller, P., Zimmermann, B., Burger, K., Devaux, P.F., and Herrmann, A. (1996) Transbilayer movement of fluorescent and spin-labeled phospholipids in the plasma membrane of human fibroblasts: a quantitative approach. *J. Cell Sci.* **109**, 687–698
33. Segawa, K., Kurata, S., and Nagata, S. (2016) Human type IV P-type ATPases that work as plasma membrane phospholipid flippases and their regulation by caspase and calcium. *J. Biol. Chem.* **291**, 762–772
34. Monesterolo, N.E., Amaiden, M.R., Campetelli, A.N., Santander, V.S., Arce, C.A., Pie, J., and Casale, C.H. (2012) Regulation of plasma membrane Ca(2+)-ATPase activity by acetylated tubulin: influence of the lipid environment. *Biochim. Biophys. Acta* **1818**, 601–608
35. Struck, D.K. and Pagano, R.E. (1980) Insertion of fluorescent phospholipids into the plasma membrane of a mammalian cell. *J. Biol. Chem.* **255**, 5404–5410
36. Cantley, L.C. Jr., Josephson, L., Warner, R., Yanagisawa, M., Lechene, C., and Guidotti, G. (1977) Vanadate is a potent (Na,K)-ATPase inhibitor found in ATP derived from muscle. *J. Biol. Chem.* **252**, 7421–7423
37. Wali, R.K., Jaffe, S., Kumar, D., and Kalra, V.K. (1988) Alterations in organization of phospholipids in erythrocytes as factor in adherence to endothelial cells in diabetes mellitus. *Diabetes* **37**, 104–111
38. Chao, Y., Chan, W.K., Birkhofer, M.J., Hu, O.Y., Wang, S.S., Huang, Y.S., Liu, M., Whang-Peng, J., Chi, K.H., Lui, W.Y., and Lee, S.D. (1998) Phase II and pharmacokinetic study of paclitaxel therapy for unresectable hepatocellular carcinoma patients. *Br. J. Cancer* **78**, 34–39
39. Gianni, L., Kearns, C.M., Giani, A., Capri, G., Vigano, L., Lacatelli, A., Bonadonna, G., and Egorin, M.J. (1995) Nonlinear pharmacokinetics and metabolism of paclitaxel and its pharmacokinetic/pharmacodynamic relationships in humans. *J. Clin. Oncol.* **13**, 180–190
40. Ohtsu, T., Sasaki, Y., Tamura, T., Miyata, Y., Nakanomyo, H., Nishiwaki, Y., and Saijo, N. (1995) Clinical pharmacokinetics and pharmacodynamics of paclitaxel: a 3-hour infusion versus a 24-hour infusion. *Clin. Cancer Res.* **1**, 599–606
41. Lang, P.A., Huober, J., Bachmann, C., Kempe, D.S., Sobiesiak, M., Akel, A., Niemoeller, O.M., Dreischer, P., Eisele, K., Klarl, B.A., Gulbins, E., Lang, F., and Wieder, T. (2006) Stimulation of erythrocyte phosphatidylserine exposure by paclitaxel. *Cell Physiol. Biochem.* **18**, 151–164

42. Barber, L.A., Palascak, M.B., Qi, X., Joiner, C.H., and Franco, R.S. (2015) Activation of protein kinase C by phorbol ester increases red blood cell scramblase activity and external phosphatidylserine. *Eur. J. Haematol.* **95**, 405–410
43. Robinson, J.M. and Vandre, D.D. (1995) Stimulus-dependent alterations in macrophage microtubules: increased tubulin polymerization and detyrosination. *J. Cell Sci.* **108**, 645–655
44. Chen, Y.M., Perng, R.P., Lee, Y.C., Shih, J.F., Lee, C.S., Tsai, C.M., and Whang-Peng, J. (2002) Paclitaxel plus carboplatin, compared with paclitaxel plus gemcitabine, shows similar efficacy while more cost-effective: a randomized phase II study of combination chemotherapy against inoperable non-small-cell lung cancer previously untreated. *Ann. Oncol.* **13**, 108–115
45. Kourousis, C., Kakolyris, S., Androulakis, N., Heras, P., Vlachonicolis, J., Vamvakas, L., Vlata, M., Hatzidaki, D., Samonis, G., and Georgoulias, V. (1998) Salvage chemotherapy with paclitaxel, vinorelbine, and cisplatin (PVC) in anthracycline-resistant advanced breast cancer. *Am. J. Clin. Oncol.* **21**, 226–232
46. Briglia, M., Fazio, A., Faggio, C., and Lang, F. (2015) Triggering of Suicidal Erythrocyte Death by Zosuquidar. *Cell Physiol. Biochem.* **37**, 2355–2365
47. Briglia, M., Fazio, A., Faggio, C., Laufer, S., Alzoubi, K., and Lang, F. (2015) Triggering of suicidal erythrocyte death by ruxolitinib. *Cell Physiol. Biochem.* **37**, 768–778
48. Fazio, A., Briglia, M., Faggio, C., Alzoubi, K., and Lang, F. (2015) Oxaliplatin induced suicidal death of human erythrocytes. *Cell Physiol. Biochem.* **37**, 2393–2404
49. Luan, Y-y., Liu, Y., Liu, X-y., Yu, B-j., Chen, R-l., Peng, M., Ren, D., Li, H-l., Huang, L., Liu, Y., Li, J-x., Feng, Y-w., and Wu, M. (2020) Coronavirus disease 2019 (COVID-19) associated coagulopathy and its impact on outcomes in Shenzhen, China: a retrospective cohort study. *Thromb. Res.* **195**, 62–68
50. Zhou, F., Yu, T., Du, R., Fan, G., Liu, Y., Liu, Z., Xiang, J., Wang, Y., Song, B., Gu, X., Guan, L., Wei, Y., Li, H., Wu, X., Xu, J., Tu, S., Zhang, Y., Chen, H., and Cao, B. (2020) Clinical course and risk factors for mortality of adult inpatients with COVID-19 in Wuhan, China: a retrospective cohort study. *Lancet* **395**, 1054–1062
51. Bitbol, M., Fellmann, P., Zachowski, A., and Devaux, P.F. (1987) Ion regulation of phosphatidylserine and phosphatidylethanolamine outside-inside translocation in human erythrocytes. *Biochim. Biophys. Acta* **904**, 268–282
52. Woon, L.A., Holland, J.W., Kable, E.P., and Roufogalis, B.D. (1999) Ca2+ sensitivity of phospholipid scrambling in human red cell ghosts. *Cell Calcium* **25**, 313–320
53. Rivelli, J.F., Ochoa, A.L., Santander, V.S., Nigra, A., Previtali, G., and Casale, C.H. (2018) Regulation of aldose reductase activity by tubulin and phenolic acid derivates. *Arch. Biochem. Biophys.* **654**, 19–26